Figure S1A
(related to Figure 1)

Ikegami and Lieb

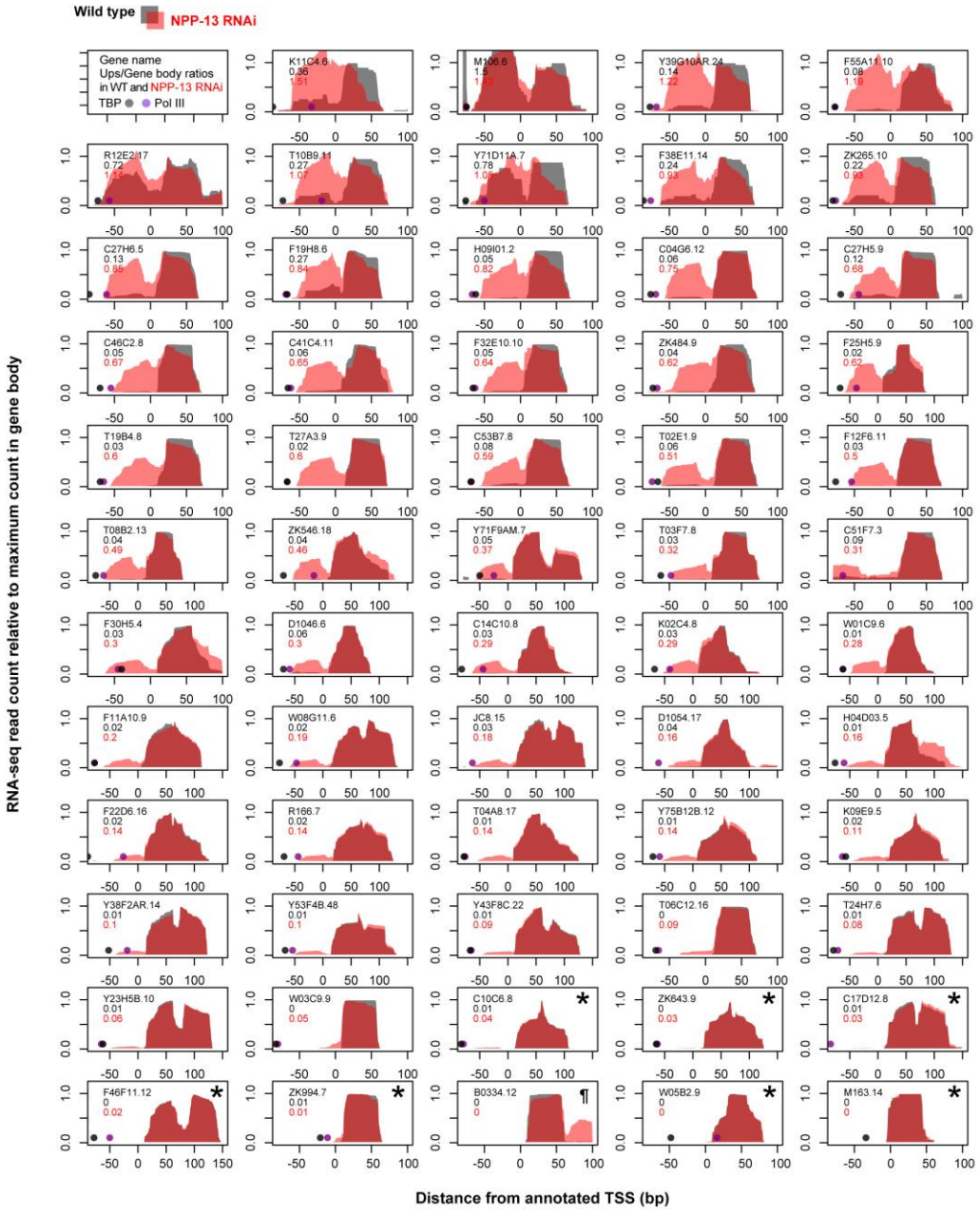

Figure S1B
(related to Figure 1)

Ikegami and Lieb

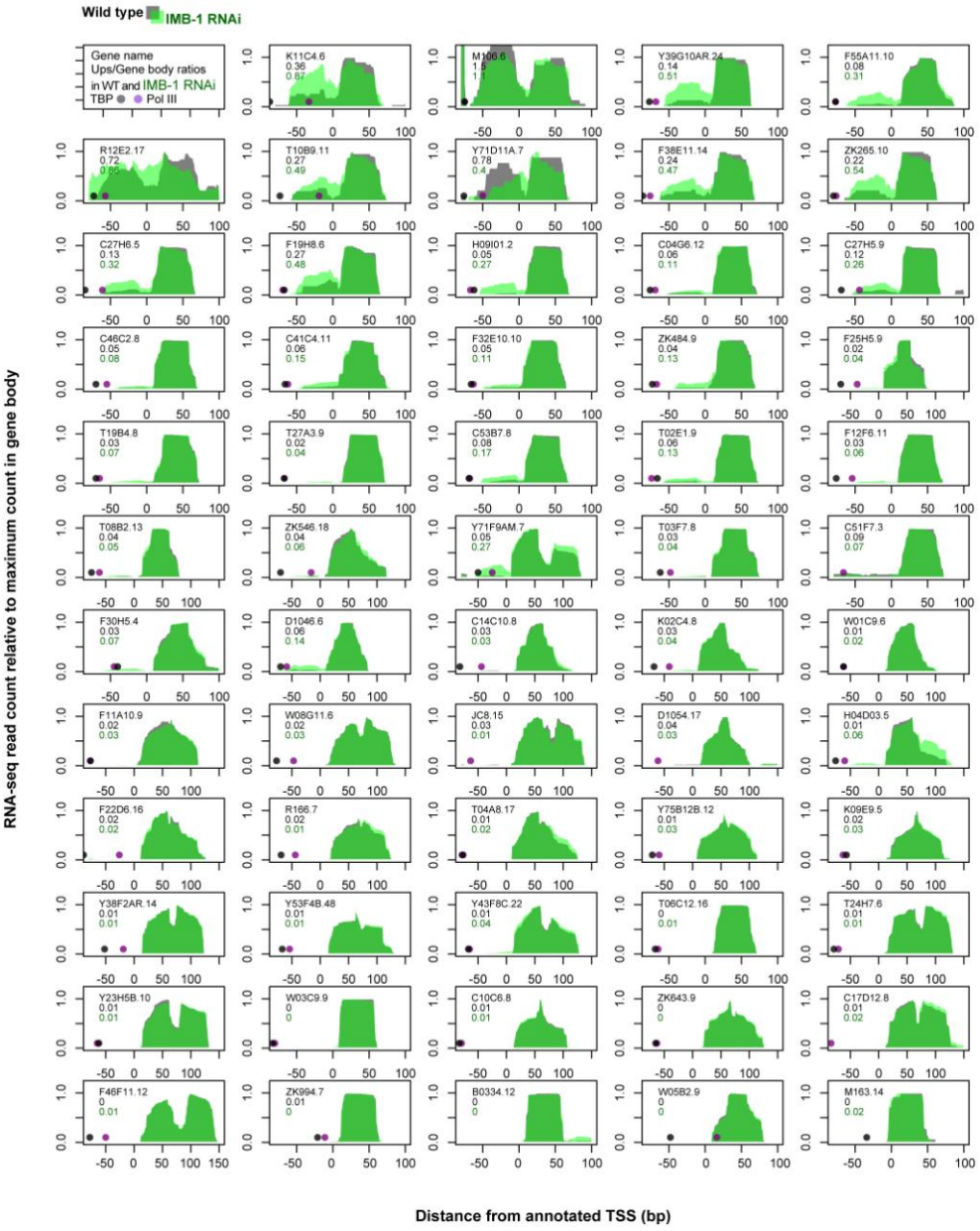

Figure S1. RNA-seq signal profiles at all Pol III-snoRNA genes (related to Figure 1)
(A) RNA-seq signal profiles of NPP-13 knockdown embryos (red) on top of the wild type profile (gray) as shown in main Figure 1C. Numbers indicate the ratio of the maximum RNA-seq read count in the upstream region (-50 bp to -10 bp of aTSS) to that in the gene body for wild type (black) and NPP-13 knockdown profiles (red). The positions of Pol III and TBP ChIP-seq read count maxima (Figure 3E) are also shown to indicate the transcription initiation site. Asterisks indicate genes without upstream RNA signals in NPP-13 knockdown embryos (the ratio < 0.05). *B0334.12* gene (pilcrow) is apparently mis-annotated in the reverse orientation.
(B) Same as (A), but RNA-seq signal profiles of IMB-1 knockdown embryos (green) are shown.

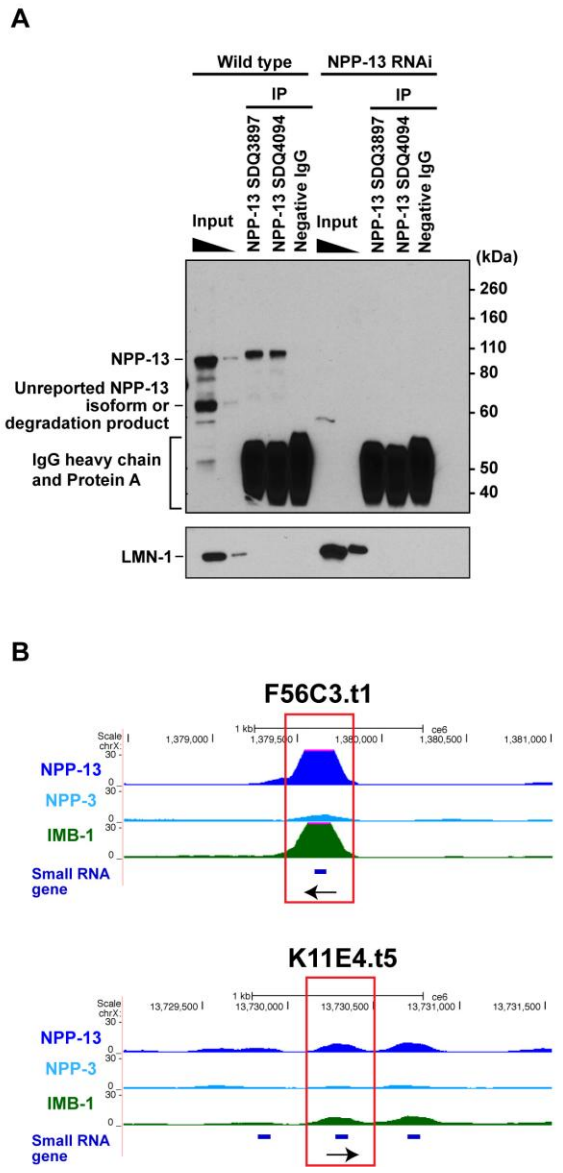

Figure S2. Validation of NPP-13 antibodies and ChIP-seq profiles at tRNA loci (related to Figure 2)

(A) Validation of anti-NPP-13 antibodies used in ChIP. Proteins immunoprecipitated with two NPP-13 antibodies (SDQ3897 and SDQ4094) in wild type and NPP-13 knockdown embryo extracts were analyzed by western blotting using another NPP-13 antibody (JL00007). In the input lanes, 3% and 0.6% of the input extracts used in ChIP were loaded. In IP lanes, 5% of the immunoprecipitants were loaded. Western blotting with anti-LMN-1 antibody (anti-nuclear lamina, SDQ2349) serves as a loading control. Wild type embryos were treated with an empty RNAi vector in parallel with NPP-13 knockdown. Note also that NPP-13 protein is effectively depleted upon NPP-13 knockdown.

(B) ChIP-seq profiles of the two tRNA loci that show 3' processing defect upon NPP-13 knockdown.

Figure S3
(related to Figures 3 and 4)

Ikegami and Lieb

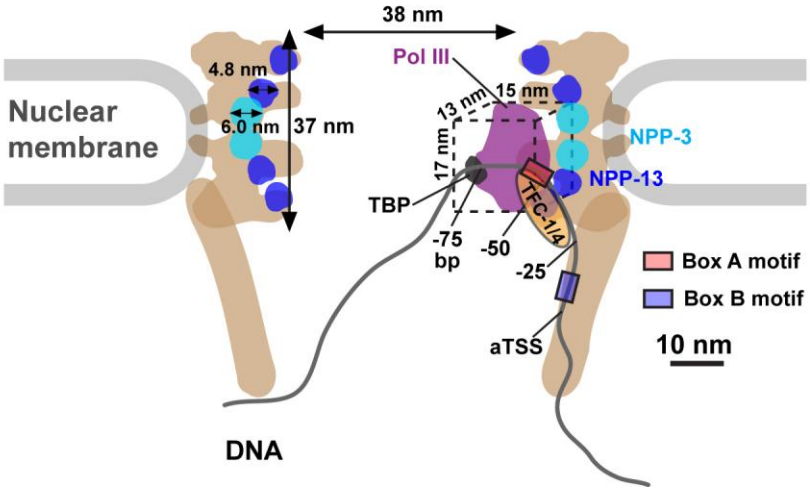

Figure S3. Scaled cartoon depicting the RNA Pol III machinery in the nuclear pore (related to Figure 3 and 4)

This highly schematic picture illustrates a hypothetical way in which the RNA Polymerase III machinery is situated in the nuclear pore. Note that the nuclear pore (Alber et al., 2007a), NPP-13 and NPP-3 (Alber et al., 2007b), and the Pol III pre-initiation complex (Fernández-Tornero et al., 2010) are depicted to the scale based on the previous studies in *S. cerevisiae*.

SUPPLEMENTAL EXPERIMENTAL PROCEDURES

Antibody

Antibodies used in ChIP experiments are listed in **Table S4**. Affinity-purified rabbit polyclonal antibodies for NPP-13 (SDQ3897 and SDQ4094; aa 667-766), IMB-1 (SDQ4154 and SDQ4155; aa 763-862), Pol III (SDQ4663; aa 1297-1396 of WormBase name RPC-1), TBP (SDQ0839; aa 16-115 of WormBase name TBP-1), TFC-1 (SDQ4526; aa 122-221 of WormBase name TFTC-5), TFC-4 (SDQ4470; aa 62-161 of WormBase name TFTC-3), Pol II (SDQ2357 and SDQ2358; aa 1460-1559 of WormBase name AMA-1) and LMN-1 (SDQ2349; aa 464-562) were generated at SDIX (Delaware, USA). SDIX antibodies are available from Novus Biologicals (Colorado, USA). Negative control IgG (Abcam ab46540; Massachusetts, USA) and anti-H3K4me3 antibody (Wako Chemicals #305-34819; Virginia, USA) are also commercially available. Affinity-purified rabbit polyclonal anti-NPP-13 antibody (JL00007; aa 12-203) used in western blotting was generated at Covance (New Jersey, USA). The anti-NPP-13 affinity-purified rabbit polyclonal antibody used in immunofluoresence and two anti-NPP-3 rabbit polyclonal antisera (SY1539 and SY1540) were described by (Hachet et al., 2012).

ChIP-seq and ChIP-chip

The ChIP procedure was detailed in (Ikegami et al., 2010). The *C. elegans* N2 strain mixed-stage embryos were harvested from the gravid adults by hypochlorite treatment and then cross-linked in 2% formaldehyde for 30 min at 25ºC. Chromatin extract was prepared by sonication in FA buffer (50 mM HEPES/KOH pH 7.5, 1 mM EDTA, 1% Triton X-100, 0.1% sodium deoxycholate; 150 mM NaCl). Five to ten micrograms of antibodies were immobilized on sepharose beads and incubated with the chromatin extract for >12 hours at 4ºC. After washing the immunoprecipitants followed by RNase treatment and reverse-crosslinking, DNA were extracted and purified. For ChIP-seq, DNA were ligated to single-end sequencing adapters and sequenced by Illumina Genome Analyzer II or Hi-seq instruments (Illumina, California, USA). Sequencing reads were aligned to the *C. elegans* reference genome (ce6, WS190) using Bowtie (Langmead et al., 2009), accepting only uniquely mapped reads with up to two mismatches. We were unable to assess ChIP enrichment at 5S ribosomal RNA loci and precise ChIP maximum locations at tRNA genes due to their high copy number. For ChIP-chip, ChIP DNA were amplified by ligation-mediated PCR and hybridized to a *C. elegans* whole-genome tiling microarray designed on the ce4/WS170 reference genome (080922_modEncode_CE_chip_HX1, Gene Expression Omnibus (GEO) accession ID

GPL8647; NimbleGen, Wisconsin) as described previously (Ikegami et al., 2010). Hybridization signals were used in subsequent analyses.

RNAi

The N2 strain worms were arrested at the L1 larva stage in the liquid S medium for synchronization. Synchronized L1 worms were fed with a bacteria strain HB101, which do not contain induction vectors, at 20ºC for 36 hours (L4 stage). L4 worms were harvested, washed and transferred to a new S medium supplemented with a bacteria strain HT115 expressing interfering double-strand RNA from L4440 vector under IPTG (RNAi bacteria). Worms were grown with the RNAi bacteria at 20ºC until the gravid stage. Embryos were harvested from the gravid adults by hypochlorite treatment and used in experiments. In parallel, worms were fed with HT115 bacteria bearing L4440 vector without target DNA insertion (empty vector RNAi). Primers used to clone DNA regions corresponding to double-strand RNA are listed in **Table S3**.

Total RNA-seq

DNase I-treated total RNA from mixed-stage embryos were processed by Ribominus kit (cat # A10837-08, Invitrogen, California, USA) to deplete rRNA. RNA were fragmented by incubating with magnesium ion at 75ºC (Fragmentation Buffer, cat # AM8740, Ambion) and subjected to double-strand cDNA synthesis using the Superscript II kit (Invitrogen). cDNA were used to generate high-throughput sequencing libraries for single-end sequencing (50 base) in the Hi-seq instrument. Reads that are uniquely mapped to the ce6/ws190 assembly were obtained using Tophat (Trapnell et al., 2009) allowing up to two mismatches and used in subsequent analyses. For visualization at multi-copy tRNA loci (Figure 1K), we used Bowtie's "--best --strata" option to select a single location with the best alignment quality when reads can be aligned to more than a single location.

Northern blotting and RT-PCR

For Northern blotting, total RNA extracted from *C. elegans* embryos were separated by polyacrylamide gel electrophoresis (PAGE) and detected by radiolabeled single-strand DNA probes. For RT-PCR, single-strand cDNA were synthesized from DNase I-treated total RNA using Random Primer (Invitrogen), and PCR products were separated by PAGE and visualized by ethidium bromide staining. Probe and primer sequences are listed in **Table S3**.

Co-immunoprecipitation

Cross-linked protein extract prepared for ChIP was used for co-immunoprecipitation. Five to ten micrograms of antibodies were immobilized on sepharose beads and incubated with the chromatin extract for >12 hours at 4ºC. Immunoprecipitants were washed with FA buffer 5 times at room temperature. Proteins were eluted from the beads and analyzed by Western Blotting as previously described (Ikegami et al., 2010).

Immunofluorescence

Mixed-stage embryos were collected from gravid worms by hypochlorite treatment and then fixed in 4% paraformaldehyde solution for 15 min at 25ºC. After one freeze-thaw cycle, embryos were blocked with PBST (PBS, 0.1% Tween 20) containing 20% goat serum. Embryos were incubated with NPP-13 antibody diluted 1:50 in the blocking buffer for 1 hour at 25 ºC. The immuno-complex was fluorescently labeled by an Alexa 488-conjugated secondary antibody. Fluorescent signals were captured using a TCS SP2 laser scanning confocal microscope with a 63x/1.47 NA objective lens (Leica Microsystems, Bannockburn, IL, USA).

Data analysis and visualization

ChIP-seq reads were extended to the original DNA fragment size estimated computationally as the distance between positive- and negative-strand reads with the highest cross-correlation. RNA-seq reads were used without extension. Using 'coverageBed' function in Bedtools (Quinlan and Hall, 2010) and 'basealigncount' function in Zinba (Rashid et al., 2011), per-base counts of extended ChIP-seq reads or RNA-seq reads were computed. Maximum counts and their positions were extracted from the per-base count vectors above using a custom Perl script. The Gaussian density estimate of the maximum positions was computed using 'density' function in R. For ChIP-chip data, hybridization signals were processed by the MA2C program (Song et al., 2007), and the genomic coordinates of MA2C scores were shifted to the ce6/WS190 genome using liftOver algorithm downloaded from the UCSC genome browser (http://genome.ucsc.edu/). ChIP data were visualized using the UCSC genome browser. RNA-seq DCPM (depth of coverage per base per million reads) calculation was performed essentially as described by (Hillier et al., 2009), except that all mapped reads, instead of rRNA-filtered total reads, were used for the denominator. All custom Perl scripts are available upon request.

NPP-13-associated sites

NPP-13-enriched sites were identified by MACS1.4 algorithm (Zhang et al., 2008) for ChIP-seq or by MA2C algorithm (Song et al., 2007) for ChIP-chip. Under a ChIP-seq p-value threshold of

less than 10^{-50} and a ChIP-chip FDR threshold less than 5%, 223 sites were identified in both applications and defined as NPP-13 associated sites.

'Pol III-target' snoRNA gene

Since our ChIP showed that some snoRNA genes exhibit strong Pol III enrichment despite the lack of apparent Box A/B motifs, we used binding levels of Pol III, instead of the motif instance, to identify Pol III-target snoRNA genes. We assumed that all Pol III-target snoRNA genes should show high levels of Pol III binding because essentially all snoRNA genes are highly expressed (**Figure 4D**). We defined a snoRNA gene to be Pol III-target when the gene possesses more than 100 Pol III ChIP-seq reads in a 200 bp region centered on the annotated TSS consistently in two biological replicates (**Figure 1I**). Out of the total 138 annotated snoRNA genes, this threshold identified 59 Pol III-target snoRNA genes. The rest of 79 snoRNA genes were defined as Pol II-targets. A previous motif-based analysis predicted 39 snoRNA genes that are transcribed by RNA Polymerase III (Deng et al., 2006). Of the 39 snoRNA genes, 38 are included in the 59 Pol III-target snoRNA genes we defined. The remaining 1 snoRNA gene (chrX:1,891,504-1,891,624) was not found in the annotation we used (ce10/WS220). Note that because each Pol III-target snoRNA gene is unique, we were able to quantitatively measure sequencing signals for each base of the snoRNA genes.

Motif analysis

The *de novo* motif discovery program MEME-ChIP (Machanick and Bailey, 2011) was used to search for DNA motifs at snoRNA loci. For each NPP-13-associated site, the presence of Box A and B motifs was re-examined by a motif search program FIMO (Grant et al., 2011) within 100 bp centered on the peak summit.

Gene annotation

We used gene annotations on the ce10/WS220 reference genome downloaded from WormMart (http://caprica.caltech.edu:9002/biomart/martview/). Using liftOver algorithm, the coordinates of the annotations were shifted to the ce6/WS190 genome, on which ChIP-seq and RNA-seq signals were mapped. SL1 splice sites were obtained from (Allen et al., 2011).

SUPPLEMENTAL REFERENCES

Alber, F., Dokudovskaya, S., Veenhoff, L.M., Zhang, W., Kipper, J., Devos, D., Suprapto, A., Karni-Schmidt, O., Williams, R., Chait, B.T., et al. (2007a). The molecular architecture of the nuclear pore complex. Nature *450*, 695–701.

Alber, F., Dokudovskaya, S., Veenhoff, L.M., Zhang, W., Kipper, J., Devos, D., Suprapto, A., Karni-Schmidt, O., Williams, R., Chait, B.T., et al. (2007b). Determining the architectures of macromolecular assemblies. Nature *450*, 683–694.

Allen, M.A., Hillier, L.W., Waterston, R.H., and Blumenthal, T. (2011). A global analysis of C. elegans trans-splicing. Genome Research *21*, 255–264.

Deng, W., Zhu, X., Skogerbø, G., Zhao, Y., Fu, Z., Wang, Y., He, H., Cai, L., Sun, H., Liu, C., et al. (2006). Organization of the Caenorhabditis elegans small non-coding transcriptome: genomic features, biogenesis, and expression. Genome Research *16*, 20–29.

Fernández-Tornero, C., Böttcher, B., Rashid, U.J., Steuerwald, U., Flörchinger, B., Devos, D.P., Lindner, D., and Müller, C.W. (2010). Conformational flexibility of RNA polymerase III during transcriptional elongation. Embo J *29*, 3762–3772.

Grant, C.E., Bailey, T.L., and Noble, W.S. (2011). FIMO: scanning for occurrences of a given motif. Bioinformatics *27*, 1017–1018.

Hachet, V., Busso, C., Toya, M., Sugimoto, A., Askjaer, P., and Gönczy, P. (2012). The nucleoporin Nup205/NPP-3 is lost near centrosomes at mitotic onset and can modulate the timing of this process in C. elegans embryos. Mol Biol Cell *23*, 3111–3121.

Hillier, L.W., Reinke, V., Green, P., Hirst, M., Marra, M.A., and Waterston, R.H. (2009). Massively parallel sequencing of the polyadenylated transcriptome of C. elegans. Genome Research *19*, 657–666.

Ikegami, K., Egelhofer, T.A., Strome, S., and Lieb, J.D. (2010). Caenorhabditis elegans chromosome arms are anchored to the nuclear membrane via discontinuous association with LEM-2. Genome Biology *11*, R120.

Langmead, B., Trapnell, C., Pop, M., and Salzberg, S.L. (2009). Ultrafast and memory-efficient alignment of short DNA sequences to the human genome. Genome Biology *10*, R25.

Machanick, P., and Bailey, T.L. (2011). MEME-ChIP: motif analysis of large DNA datasets. Bioinformatics *27*, 1696–1697.

Quinlan, A.R., and Hall, I.M. (2010). BEDTools: a flexible suite of utilities for comparing genomic features. Bioinformatics *26*, 841–842.

Rashid, N.U., Giresi, P.G., Ibrahim, J.G., Sun, W., and Lieb, J.D. (2011). ZINBA integrates local covariates with DNA-seq data to identify broad and narrow regions of enrichment, even within amplified genomic regions. Genome Biology *12*, R67.

Song, J.S., Johnson, W.E., Zhu, X., Zhang, X., Li, W., Manrai, A.K., Liu, J.S., Chen, R., and Liu, X.S. (2007). Model-based analysis of two-color arrays (MA2C). Genome Biology *8*, R178.

Trapnell, C., Pachter, L., and Salzberg, S.L. (2009). TopHat: discovering splice junctions with RNA-Seq. Bioinformatics *25*, 1105–1111.

Zhang, Y., Liu, T., Meyer, C.A., Eeckhoute, J., Johnson, D.S., Bernstein, B.E., Nusbaum, C., Myers, R.M., Brown, M., Li, W., et al. (2008). Model-based analysis of ChIP-Seq (MACS). Genome Biology *9*, R137.